PHYSICAL REVIEW LETTERS

Orbital Ordering and Magnetic Field Effect in MnV$_2$O$_4$

T. Suzuki,[1] M. Katsumura,[1] K. Taniguchi,[2] T. Arima,[2] and T. Katsufuji[1,3]

[1]*Department of Physics, Waseda University, Tokyo 169-8555, Japan*
[2]*Institute of Multidisciplinary Research for Advanced Materials, Tohoku University, Sendai 980-8577, Japan*
[3]*Kagami Memorial Laboratory for Material Science and Technology, Waseda University, Tokyo 169-0051, Japan*

We studied the structural properties of an orbital-spin-coupled spinel oxide, MnV$_2$O$_4$, mainly by single-crystal x-ray diffraction measurement. It was found that a structural phase transition from cubic to tetragonal and ferrimagnetic ordering occur at the same temperature (T_s, $T_N = 57$ K). The structural phase transition was induced also by magnetic field above T_s. In addition, magnetic-field-induced alignment of tetragonal domains results in large magnetostriction below T_s. We also found that the structural phase transition is caused by the antiferro-type ordering of the V t_{2g} orbitals.

PACS numbers: 75.80.+q, 61.10.Nz, 75.10.−b, 75.50.Gg

Orbital degeneracy of d electrons plays important roles for various properties in transition-metal oxides. When the number of d electrons or holes in a transition metal are smaller than the number of degeneracy of d orbitals, the d electrons have the freedom of which orbitals to occupy. In such a case, the occupation of d orbitals at one site often has a correlation with the occupation at the next site, meaning that orbitals at neighboring sites have an interaction. Thus, analogously to spin ordering, the orbital degree of freedom can order at low temperatures (orbital ordering), and particular orbitals are occupied at each site. An interesting aspect of the orbital degree of freedom is that it is often coupled with the spin degree of freedom. This coupling arises from the fact that whether the same orbitals or different orbitals are occupied at neighboring sites is strongly influenced by whether the neighboring spins are aligned to the same direction or the opposite direction [1].

Possibility of orbital ordering has been discussed in perovskite manganites for doubly degenerate e_g orbitals of Mn ions [2,3], and perovskite [4,5] and spinel vanadates [6–8] for triply degenerate t_{2g} orbitals of V ions. Among them, spinel vanadates occupy a peculiar position, since they take a perfect cubic structure in the absence of orbital ordering, in contrast to perovskite manganites and perovskite vanadates, in which the crystal structure is distorted (the so-called GdFeO$_3$ distortion) even without orbital ordering. Since such a built-in distortion causes complications in the study of orbital physics, spinel vanadates are more suitable to the detailed study.

Various studies have been done on spinel vanadates with V^{3+} ($3d^2$) in the octahedral site (ZnV$_2$O$_4$ [6–8], MnV$_2$O$_4$ [9–11]) so far. In this series of compounds, there is antiferromagnetic (ZnV$_2$O$_4$) or ferrimagnetic (MnV$_2$O$_4$) ordering, which are dominated by the direct t_{2g}-t_{2g} interaction between neighboring V^{3+} spins ($S = 1$), or by the superexchange interaction through the oxygen $2p$ orbital between V^{3+} and Mn^{2+} ($S = 5/2$) spins [Fig. 1(a)], respectively, and a structural phase transition into a tetragonal phase, presumably induced by the ordering of V

orbitals. However, experimental studies to microscopically understand the orbital ordering and the orbital-spin coupling have yet to be done. For example, direct evidence of orbital ordering has not been obtained in spinel vanadates so far, except for a tetragonal lattice distortion at low temperatures, which only indirectly suggests the ordering of V orbitals.

In this Letter, we report the x-ray diffraction measurement as well as magnetic and strain measurement on single crystals of MnV$_2$O$_4$ with Mn^{2+} ($3d^5$) in the tetrahedral site of the spinel structure. For strain measurement, a strain gauge was attached to the (001) surface of the crystal, and the striction (ΔL) along the [110] was measured. Magnetization was measured by a SQUID magnetometer. X-ray diffraction measurements were carried out at BL-4C (without magnetic field) and BL-16A1 (with magnetic field) of the Photon Factory, KEK. A 13-keV monochromatic x ray was used in both measurements. For the measurement with magnetic field, magnetic field was applied parallel to the ω rotation axis, and the x-ray scattering vector was set perpendicular to the ω axis (the magnetic-field direction), meaning that only the plane parallel to the ω axis (the magnetic-field direction) can be detected in the measurement under magnetic field. The single crystal was attached in such a way that one principal axis is parallel to the ω axis.

Figure 1(b) shows the temperature (T) dependence of striction ($\Delta L/L$) and magnetization (M) of MnV$_2$O$_4$. As can be seen, $\Delta L/L$ of the single crystal sharply decreases at 57 K; x-ray diffraction patterns around the (440) peak are shown in Fig. 1(c). The peak is split into two peaks [(400) and (224) in the tetragonal setting] below 57 K, consistent with the tetragonal lattice distortion reported previously. (Note that the unit cell of the tetragonal phase is half of that of the cubic phase.) The lattice constants obtained from the x-ray measurement are plotted in Fig. 1(d). The absolute value of $\Delta L/L$ below 57 K ($\sim 1.5 \times 10^{-3}$) shown in Fig. 1(d) is close to $1 - (\sqrt{2}a_t + c_t)/2a_c$ ($\sim 1.8 \times 10^{-3}$), where a_t and c_t are the a and c
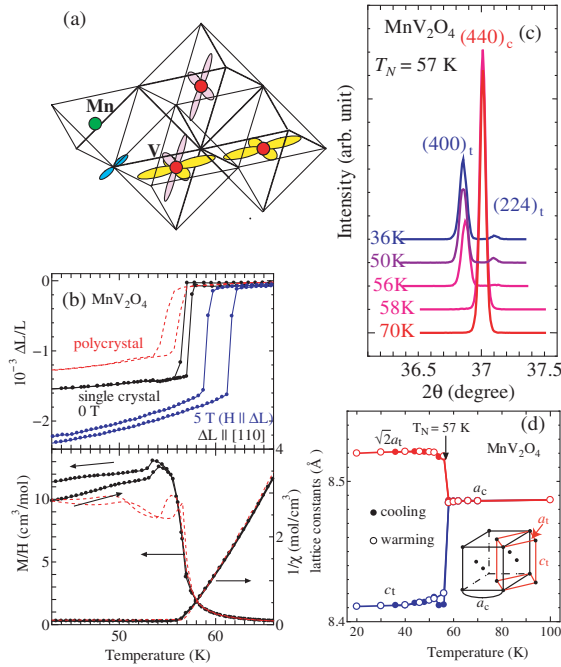
127203-1

FIG. 1 (color online). (a) Schematic picture of the crystal structure and the orbital orientations of spinel MnV_2O_4. Oxygen atoms are on the corner without circles. (b) Temperature dependence of striction under 0 T and 5 T (upper panel), magnetization under 1000 G (lower panel, left axis), and inverse magnetic susceptibility (lower panel, right axis). Solid lines are for single crystals whereas dashed lines are for polycrystalline samples. (c) Temperature dependence of the x-ray diffraction of the MnV_2O_4 single crystal around the (440) peak in the cubic setting. (d) Temperature dependence of lattice constants.

lattice constants in the tetragonal phase and a_c the lattice constant in the cubic phase. This means that the c axis in the tetragonal phase, which is shorter than the cubic lattice constant, is preferably oriented along the bonding plane between the strain gauge and the sample, presumably because of the compressive stress applied to the bonding plane.

As also shown in Fig. 1(b), the magnetization sharply increases (or the extrapolation of the inverse magnetization crosses the x axis) at the same temperature of the structural phase transition (~ 57 K). This indicates that the structural phase transition and the ferrimagnetic ordering, where the Mn^{2+} spin and the V^{3+} spin are aligned to the opposite direction [9], occur at the same temperature in single crystals of MnV_2O_4. The behaviors of polycrystalline MnV_2O_4 are also plotted by dashed lines in Fig. 1(b). The T dependence of M is almost the same between single and polycrystalline samples (except for the height of M below T_N), but T dependence of $\Delta L/L$ is quite different. Namely, $\Delta L/L$ shows only the onset of a gradual decrease at $T_N = 57$ K in polycrystalline samples, in contrast to the sharp change in single crystals. Such a gradual temperature dependence of the structural anomaly in polycrystalline samples can be attributed to the effect of disorder, and it is likely that in the T range where $\Delta L/L$ varies (between 53

and 57 K in the cooling run for polycrystalline samples), both the cubic and the tetragonal phases coexist, and their volume fraction varies with temperature.

The T dependence of $\Delta L/L$ under 5 T is also plotted in Fig. 1(b). As can be seen, a sharp decrease of $\Delta L/L$ shifts to higher temperatures with applied magnetic field. Magnetic-field (H) dependence of $\Delta L/L$ and M are shown in Fig. 2(a). $\Delta L/L$ sharply decreases with applied magnetic field immediately above T_N, indicating a structural anomaly under magnetic field. Associated with this structural anomaly, $M(H)$ curves also show an anomaly almost at the same magnetic field [Fig. 2(b)]. These experimental results clearly indicate the correlation between the crystal structure and magnetism in this compound, in such a way that the state with a larger M favors the distorted crystal structure and vice versa.

Figure 2(c) shows the variation of x-ray diffraction patterns around the (800) peak under various magnetic fields at 59 K ($> T_N, T_s$). The peak at 52.6°, corresponding to the cubic (800) peak, jumps to 52.4°, corresponding to the tetragonal (440) peak, above 4 T. This experimental result gives the direct evidence that the crystal structure is switched from cubic to tetragonal with applied magnetic field.

In the tetragonal phase, the cubic (800) peak should be split into the (440) peak and (008) peak. However, no tetragonal (008) peak, which should appear at the position shown by the arrow in Fig. 2(c), was observed. Such absence of diffraction peaks in the tetragonal phase suggests that the tetragonal phase has a single-domain structure under magnetic field. To see how such a tetragonal
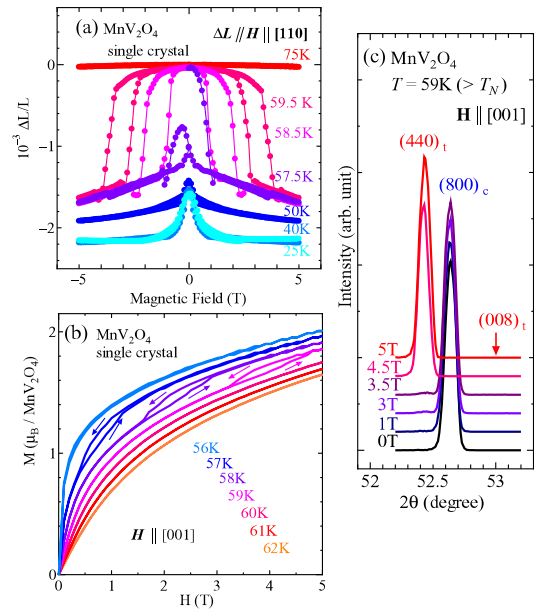

FIG. 2 (color online). (a) Magnetic-field dependence of striction at various temperatures. (b) Magnetic-field dependence of magnetization at various temperatures. (c) Magnetic-field dependence of x-ray diffraction of the MnV_2O_4 single crystal around the (800) peak in the cubic setting.

domain structure behaves under magnetic field, the (840) peak in the cubic setting was monitored below the structural transition temperature (56 K $< T_N$, T_s = 57 K) with increasing magnetic field. When the cubic crystal is distorted into a tetragonal structure, there appear three domains depending on the direction of the c axis, as shown in Fig. 3(b). Thus, the cubic (840) peak should be split into the (620), (444), and (228) peaks in the tetragonal phase, arising from domain 1, 2, and 3, respectively, as shown in Fig. 3(b). As seen in Fig. 3(a), the (444) and (228) peaks arising from domain 2 and 3 can be observed in the absence of magnetic field. However, these peaks disappear and only the (620) peak arising from domain 1, where the c axis is oriented to the magnetic-field direction, appears under magnetic field. This clearly indicates that the sample becomes a single-domain structure with the c axis parallel to the applied magnetic field.

Such a domain alignment with magnetic field leads to large magnetostriction. As shown in Fig. 3(c), there appears large positive magnetostriction when magnetic field is applied perpendicular to the plane of the strain gauge. This can be explained by the following two-step scenario: (1) the short axis (c axis) is preferably oriented along the plane of the strain gauge without magnetic field, but (2) when the magnetic field is applied perpendicular to the plane, the short c axis is flipped to that direction, and longer axes are left along the plane in its consequence. However, the behavior of magnetostriction is not quantitatively consistent with the result of x-ray diffraction; the change of $\Delta L/L$ with magnetic field is smaller than that expected for the untwined tetragonal structure under magnetic field ($\sim 6 \times 10^{-3}$), particularly at high temperatures. This discrepancy can also be attributed to the compressive stress applied to the bonding plane with the strain gauge, which disturbs the flip of the c axis with magnetic field.
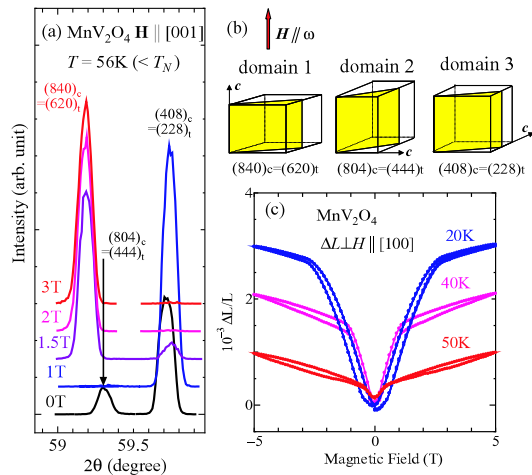
Since the tetragonal domain is perfectly aligned with magnetic field even immediately below the transition temperature (56 K) in the x-ray diffraction measurement, which was done free from strong stress, the temperature dependence of magnetostriction shown in Fig. 3(c) is dominated by the competition between the compressive stress on the bonding plane and the energy gain by aligning the c axis along the magnetic field, which increases with the evolution of M.

The structural phase transition observed in the present MnV_2O_4 is the same as that of ZnV_2O_4 in that the c axis is shorter than the a, b axis. As has been pointed out already, this distortion splits the triply degenerate t_{2g} orbitals of vanadium ions into a nondegenerate xy orbital at lower energy and doubly degenerate yz and zx orbitals at higher energy, and thus, degeneracy is not lifted when two electrons are accommodated in these t_{2g} orbitals. To lift the degeneracy of the second electron in the degenerate yz and zx orbitals, Tsunetsugu and Motome proposed a model of "antiferro-orbital" ordering for ZnV_2O_4 [12], in which the yz and the zx orbitals are alternately occupied along the c axis (Fig. 4). This orbital ordering breaks the mirror symmetries at the center of two V sites in the same xy plane as well as the diamond-glide symmetries (space group $I4_1/a$). Khomskii and Mizokawa proposed an "orbital-Peierls" model [13], in which the yz and zx orbital are aligned as yz-yz-zx-zx chains along the [101] or [011] direction (in the cubic setting). In this structure, not only

FIG. 3 (color online). (a) Magnetic-field dependence of x-ray diffraction of the MnV_2O_4 single crystal at 56 K ($< T_N$) around the (840) peak in the cubic setting, split as the (620), (444), and (228) peaks in the tetragonal setting. (b) Schematic picture of three tetragonal domains and the (804) planes. (c) Magnetic-field dependence of striction at various temperatures.
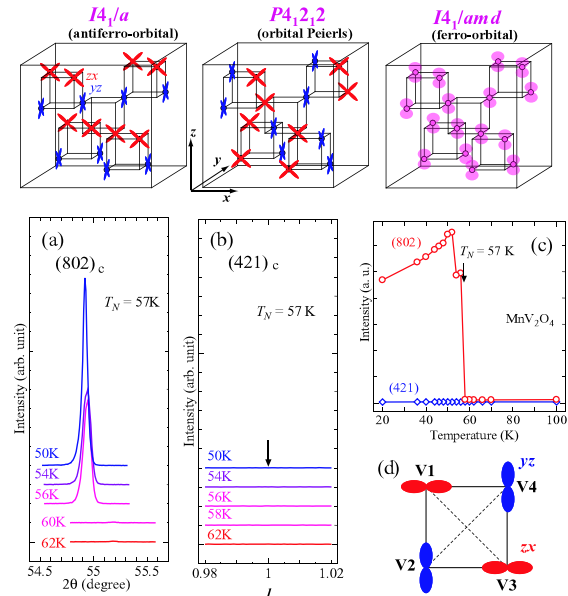

FIG. 4 (color online). Upper panel: three theoretical models of orbital ordering in spinel vanadate. Lower panel: temperature dependence of x-ray diffraction of the MnV_2O_4 single crystal around (a) the (802) peak in the cubic setting, and (b) the (421) peak in the cubic setting, and (c) the temperature dependence of their intensities. (d) Schematic picture of t_{2g} orbitals in one tetrahedron. $V1$ and $V3$ are on the same layer, which is above the layer containing $V2$ and $V4$.

the mirror planes and the glide planes, but also the face center symmetry in the spinel structure is missing (space group $P4_12_12$). Tchernyshyov proposed a model of "ferro-orbital" ordering for ZnV_2O_4 [14], in which single-ion spin-orbit coupling is taken into account to lift the degeneracy, and the mixed state of the yz and zx orbitals at each V is occupied by the second electron. This model does not induce further lowering of the crystal symmetry except for a tetragonal distortion (space group $I4/amd$).

So far, diffraction measurements have been done only on the powder samples of ZnV_2O_4, and no extra peak has been observed, seemingly consistent with the ferro-orbital model. However, powder diffraction measurement cannot detect the peaks with small intensities (typically less than 10^{-4} times of the fundamental peaks), and the diffraction measurement on single crystals is indispensable to know which of these three models is appropriate. We investigate the T dependence of the (802) peak and the (421) peak (in the cubic setting) for a MnV_2O_4 single crystal. These peaks are absent in the cubic spinel structure by the diamond-glide symmetry and the face center symmetry, respectively, and this extinction rule holds even in the tetragonal phase with space group $I4/amd$. The diffraction patterns around the (802) and (421) peaks are shown in Fig. 4(a) and 4(b). As can be seen, the (802) peak appears below the T_N, T_s, but the (421) does not. This result indicates that the diamond glides are missing while the face center symmetry (the body center symmetry in the tetragonal setting) still exists in the tetragonal phase. Therefore, the present experimental result indicates the space group $I4_1/a$, and supports the antiferro-orbital model for MnV_2O_4 (Fig. 4, upper left).

The present experimental results can be summarized in such a way that ferrimagnetic ordering, where the Mn spins and the V spins are aligned to the opposite direction, and the antiferro-orbital ordering, where the yz and the zx orbitals are alternately occupied along the c axis, occur at the same temperature in MnV_2O_4. For simplicity, only the direct electron hopping through a σ bond between two t_{2g} orbitals of the neighboring V ions is taken into account in the following discussion. There are ferro-orbital V-V bonds, where the occupied t_{2g} states of the two V ions at the ends have a σ bond, and antiferro-orbital V-V bonds, where the occupied t_{2g} state of one V ion and the unoccupied t_{2g} state of the other V ion have a σ bond. According to the Kugel-Khomskii calculation on the spinel structure, the energy gain of the antiferro-oribtal bond is larger than the ferro-orbital bond when the neighboring spins are ferromagnetically aligned, since electron hopping is prohibited due to the Pauli principle in the ferro-oribtal bond with ferromagnetically aligned spins [12]. Thus, associated with the ferrimagnetic ordering, where the V spins are ferromagnetically aligned, the antiferro-orbital-ordered state proposed by Tsunetsugu and Motome [12], where there are four antiferro-orbital bonds [$V1$-$V3$, $V1$-$V4$, $V2$-$V3$, $V2$-$V4$ in Fig. 4(d)] in one V tetrahedron and

thus the number of the antiferro-bonds is maximized, has the lowest energy. This can explain the simultaneous ferrimagnetic and orbital ordering in zero field, as well as the magnetic-field-induced structural phase transition.

The domain alignment by magnetic field in the tetragonal phase, as shown in Fig. 3(a), can be explained in several ways. If spin anisotropy exists, i.e., V spins are preferably oriented in a certain direction of the tetragonal crystal (usually owing to single-ion spin-orbit coupling), inversely the tetragonal domain can be aligned by aligning the V spins with applied magnetic field. In MnV_2O_4, if the antiferro-orbital ordering is perfect, i.e., only the yz or zx orbital is occupied by the second electron of the V ion, then the orbital angular momentum is quenched. In this case, spin anisotropy still exists arising from the exchange process between V-V or V-Mn, plus spin-orbit coupling, though the spin anisotropy arising from such higher-order process is not very strong. Another possibility is that the antiferro-orbital ordering is not perfect, i.e., the second electron of the V ion occupies the superposition of the yz and zx orbitals (though there is a preference of them corresponding to the antiferro-orbital pattern) and thus, the angular momentum is not totally quenched for the V orbitals. Such imperfect orbital ordering is possible by taking account of not only the electron hopping through the σ bonds of the neighboring t_{2g} orbitals, but also those through other paths [15].

[1] K. I. Kugel and D. I. Khomskii, Zh. Eksp. Teor. Fiz. **64**, 369 (1973) [Sov. Phys. JETP **37**, 725 (1973)].
[2] J. B. Goodenough, Phys. Rev. **100**, 564 (1955).
[3] Y. Murakami *et al.*, Phys. Rev. Lett. **81**, 582 (1998).
[4] Y. Ren *et al.*, Nature (London) **396**, 441 (1998).
[5] M. Noguchi *et al.*, Phys. Rev. B **62**, R9271 (2000).
[6] Y. Ueda, N. Fujiwara, and H. Yasuoka, J. Phys. Soc. Jpn. **66**, 778 (1997).
[7] M. Reehuis *et al.*, Eur. Phys. J. B **35**, 311 (2003).
[8] S.-H. Lee *et al.*, Phys. Rev. Lett. **93**, 156407 (2004).
[9] R. Plumier and M. Sougi, Solid State Commun. **64**, 53 (1987).
[10] R. Plumier and M. Sougi, Physica (Amsterdam) **155B**, 315 (1989).
[11] K. Adachi, Phys. Rev. Lett. **95**, 197202 (2005).
[12] H. Tsunetsugu and Y. Motome, Phys. Rev. B **68**, 060405(R) (2003).
[13] D. I. Khomskii and T. Mizokawa, Phys. Rev. Lett. **94**, 156402 (2005).
[14] O. Tchernyshyov, Phys. Rev. Lett. **93**, 157206 (2004).
[15] Y. Motome (private communication).